

## Crystal structure of synthetic $\text{Al}_4\text{B}_2\text{O}_9$ : A member of the mullite family closely related to boralsilite

REINHARD X. FISCHER,<sup>1,\*</sup> VOLKER KAHLBERG,<sup>2</sup> DIETMAR VOLL,<sup>3</sup> KENNETH J.D. MACKENZIE,<sup>4</sup>  
MARK E. SMITH,<sup>5</sup> BERNHARD SCHNETGER,<sup>6</sup> HANS-JÜRGEN BRUMSACK,<sup>6</sup>  
AND HARTMUT SCHNEIDER<sup>1</sup>

<sup>1</sup>Fachbereich Geowissenschaften, Universität Bremen, Klagenfurter Strasse, D-28359 Bremen, Germany

<sup>2</sup>Institut für Mineralogie und Petrographie, Universität Innsbruck, Innrain 52, A-6020 Innsbruck, Austria

<sup>3</sup>Institut für Mineralogie und Kristallographie, Universität Wien—Geozentrum, Althanstrasse 14, A-1090 Wien, Austria

<sup>4</sup>School of Chemical and Physical Sciences, Victoria University of Wellington, P.O. Box 600, Wellington, New Zealand

<sup>5</sup>Department of Physics, University of Warwick, Coventry, CV4 7AL, U.K.

<sup>6</sup>Institut für Chemie und Biologie des Meeres (ICBM), Universität Oldenburg, Carl von Ossietzky Strasse, D-26111 Oldenburg, Germany

### ABSTRACT

The crystal structure of  $\text{Al}_4\text{B}_2\text{O}_9$ , synthesized from  $\text{Al}(\text{NO}_3)_3 \cdot 9\text{H}_2\text{O}$  and  $\text{B}(\text{OH})_3$  via a sol-gel process, is studied and characterized by Rietveld refinements and grid search analyses combined with  $^{11}\text{B}$  and  $^{27}\text{Al}$  MAS NMR spectroscopy. The aluminum borate with a unit-cell composition of  $\text{Al}_{32}\text{B}_{16}\text{O}_{72}$  is closely related to the boralsilite ( $\text{Al}_{32}\text{B}_{12}\text{Si}_4\text{O}_{74}$ ) structure with Si replaced by B and to mullite ( $\text{Al}_{4+2x}\text{Si}_{2-2x}\text{O}_{10-x}$ ). It crystallizes in the monoclinic space group  $C2/m$ ,  $a = 14.8056(7)$  Å,  $b = 5.5413(2)$  Å,  $c = 15.0531(6)$  Å,  $\beta = 90.913(2)^\circ$ ,  $Z = 8$  for  $\text{Al}_4\text{B}_2\text{O}_9$ . The main structural units are isolated chains of edge-sharing  $\text{AlO}_6$ -octahedra running parallel to  $\mathbf{b}$  that is a characteristic feature of the mullite-type crystal structures. The octahedral chains are crosslinked by  $\text{AlO}_4$ ,  $\text{AlO}_5$ ,  $\text{BO}_3$ , and  $\text{BO}_4$  groups with two B atoms and one O atom ( $\text{O}5'$ ) disordered on interstitial positions.  $^{27}\text{Al}$  and  $^{11}\text{B}$  NMR studies confirm the presence of sixfold (octahedral), fivefold, and fourfold (tetrahedral) coordinated Al (sixfold:[fourfold + fivefold] = ~50%:50%) and of threefold and fourfold coordinated B (~80%:20%).

**Keywords:** Aluminum borate, boron aluminate,  $\text{Al}_4\text{B}_2\text{O}_9$ , boralsilite, crystal structure, Rietveld refinement, MAS NMR spectroscopy

### INTRODUCTION

The  $\text{Al}_4\text{B}_2\text{O}_9$  phase, yet to find significant technological application, is of considerable crystal-chemical importance. It is a member of the family of aluminum borates, some of which have properties similar to mullite ( $\text{Al}_{4+2x}\text{Si}_{2-2x}\text{O}_{10-x}$ ) as noted already by Scholze (1956). Werding and Schreyer (1984, 1990, 1996) used the term “boron-mullites” for such intermediate members. Scholze (1956) indicated that  $\text{Al}_4\text{B}_2\text{O}_9$  crystallizes in an orthorhombic unit cell of unknown space group with  $a = 14.8$  Å,  $b = 15.1$  Å,  $c = 5.6$  Å, and  $Z = 8$ . Structure refinements by Mazza et al. (1992), however, yielded an orthorhombic mullite-type structure in space group  $Pbam$  with a pseudo tetragonal metric of  $a = b = 7.6717$  Å,  $c = 2.827$  Å, and  $Z = 1$ . In this paper, it is our aim to determine the correct crystal structure of  $\text{Al}_4\text{B}_2\text{O}_9$  using a combination of NMR spectroscopy and X-ray diffraction methods.

### EXPERIMENTAL METHODS

#### Sample preparation

The aluminum borate sample was synthesized following the nitrate decomposition method described by Mazza et al. (1992). Aluminum nitrate nonahydrate [ $\text{Al}(\text{NO}_3)_3 \cdot 9\text{H}_2\text{O}$ ; Fluka, lot 06274] and boric acid [ $\text{B}(\text{OH})_3$ ; Merck, lot 165] in proportions corresponding to an Al:B ratio of 1:2 were intimately mixed together with 10 wt% glycerol in a beaker. This mixture was slowly heated to 80 °C under

continuous stirring until a homogeneous solution was obtained. After heating to 110 °C, foaming of the liquid was observed and the decomposition of the nitrate started with evaporation of brownish  $\text{NO}_x$  gases. After the reaction was completed, a highly viscous, white gel formed. This gel was dried at 200 °C for 30 min and afterward crushed to a powder. The powder was further calcined at 300 °C for 2 h to remove part of the residual nitrate and organic compounds. The crystalline phase was obtained after heat-treating the calcined powder at 950 °C for 5 h.

Initial X-ray diffraction measurements showed that  $\text{B}(\text{OH})_3$  (boric acid) was present as an impurity phase remaining from the synthesis procedure. The existence of boric acid in the crystalline sample can be attributed to rehydration of non-crystalline  $\text{B}_2\text{O}_3$  by contact with humid air. Washing with deionized water at boiling temperature completely removed the boric acid as shown by subsequent X-ray diffraction analysis. Consequently, the boron content in the crystalline phase must be lower than indicated by the composition of the mixture of initial reagents that would imply an Al:B ratio of 1:2. Quantitative analysis by the Rietveld method yielded 66 wt%  $\text{Al}_4\text{B}_2\text{O}_9$  and 34 wt%  $\text{B}(\text{OH})_3$  (atomic parameters from Gajhede et al. 1986) that corresponds to 30 mol% of the aluminum borate and 70 mol% of boric acid, and consequently corresponds to an Al:B ratio of 0.44 close to the ratio of 0.5 in the initial mixture.

#### Chemical analysis

Ten milligrams of washed [ $\text{B}(\text{OH})_3$ -free] and milled material (<125  $\mu\text{m}$ ) was dissolved in an acid mixture (1 mL 40% HF, suprapure quality Merck, Germany and 0.5 mL HCl of subboiling quality, home-made) in closed teflon vessels for one hour on a hot plate at 100 °C and diluted to a volume of 50 mL. Prior to the measurement, the sample solution was diluted twofold. Diluted mono-element solutions of Alfa Aesar (Specpure, 1000 or 10000 mg/L) were used for the preparation of the calibration solutions. Scandium (1 mg/L) was used as an internal standard. The measurement was done by an ICP-OES instrument (Perkin Elmer 3000 XL) using two Al lines (396.153, 934.401 nm) and three B lines (249.772, 208.957, 208.889 nm). Precision, determined by the relative standard variation for the measurement, was better than 2% (three replicates). Accuracy was checked by two independently prepared solutions in the range of the expected concentration

\* E-mail: rfischer@uni-bremen.de

of the samples (<2%).

The material was split into two parts for two independent sample preparations. The first batch was measured twice to check the reproducibility of the results. The three analyses yielded aluminum content between 39.4 and 41.6 wt%, and a boron content between 8.1 and 8.5 wt% corresponding to Al/B ratios between 1.90 and 1.98 with a mean value of 1.95 and an experimental error of ±0.1. Consequently, the composition Al<sub>4</sub>B<sub>2</sub>O<sub>9</sub> with an Al/B ratio of 2, which is within the error margins of the chemical analyses, is assumed for all further investigations. Possible deviations from this stoichiometry are discussed in the last part of the discussion section related to the O5' position.

### X-ray data collection and Rietveld refinement procedure

X-ray data were collected on a Philips X'Pert diffractometer with a Ge monochromator in the primary beam yielding strictly monochromatic radiation resulting in very sharp X-ray reflections. Details of data collection, crystallographic data, and definitions are given in Table 1. Background values were set by hand and consecutive background points were linearly interpolated. Intensities within eight times the full width at half maximum of a peak were considered to contribute to the central reflection. Peaks below 50 °2θ were corrected for asymmetry effects using Rietveld's (1969) algorithm. The pseudo-Voigt function was used for the modeling of the peak shape, with a refinable parameter defining the Lorentzian and Gaussian character of the peaks as a function of 2θ. The Rietveld analysis (Rietveld 1969) was performed with PC-Rietveld plus (Fischer et al. 1993) and the 2004 version of the program BRASS (Birkenstock et al. 2007). Estimated standard deviations (esds) of the least squares variables are calculated as the square roots of the diagonal elements of the variance-covariance matrix multiplied by the χ factor ( $R_{wp}/R_e$ ) as discussed by Prince (1995). X-ray scattering factors in their respective valence states were taken from the *International Tables for X-ray Crystallography* (Ibers and Hamilton 1974) and the values for O<sup>2-</sup> from Hovestreydt (1983). Crystal structure drawings are done with the program STRUPLO (Fischer and Messner 2007).

### NMR spectroscopy

Solid-state multinuclear magic angle spinning (MAS) NMR experiments were carried out on the same sample as used for the Rietveld X-ray analysis. The <sup>27</sup>Al spectra were acquired at magnetic fields of 8.45, 11.7, 14.1, and 16.45 T at frequencies of 93.8, 130.3, 156.4, and 182.4 MHz, respectively, using Varian Unity, Infinity or Infinity Plus spectrometers with 4 and 5 mm Doty MAS probes spun at 12–15 kHz, and at the higher fields 3.2 and 2.5 mm Chemagnetics probes spun at 15–18 kHz were used. A short pulse of 0.5 μs (corresponding to ~π/15) and a recycle delay of 1 s were selected to prevent saturation of the signal and allow quantitative comparison between signals with different quadrupole interactions. Spectra were referenced against the AlO<sub>6</sub> resonance of Y<sub>3</sub>Al<sub>5</sub>O<sub>12</sub> at 0.7 ppm w.r.t. Al(H<sub>2</sub>O)<sub>6</sub><sup>3+</sup> (Smith and van Eck 1999). <sup>11</sup>B MAS NMR spectra were acquired at 11.7 and 14.1 T at frequencies of 160.4 and 192.55 MHz on Varian Unity and Varian-Chemagnetics Infinity spectrometers, respectively. For the 14.1 T spectra a 3.2 mm Chemagnetics probe was used spun at 13–15 kHz with a pulse of 0.7 μs (corresponding to ~π/12) and a recycle delay of 1s. Spectra were referenced against solid BPO<sub>4</sub> at -3.3 ppm w.r.t. BF<sub>3</sub>Et<sub>2</sub>O.

## RESULTS

After removing the boric acid by washing the sample, the pure boron aluminate phase was studied by NMR and X-ray diffraction methods. The <sup>11</sup>B MAS NMR results indicate that about 20% of boron is tetrahedrally coordinated and 80% is in a trigonal planar configuration. The tetrahedral site (Fig. 1d) can be fitted by a single Gaussian peak at -1.8 ppm but the more distorted trigonal site can be fitted by a second-order quadrupolar lineshape with an isotropic chemical shift of 16.3 ppm, a nuclear quadrupolar coupling constant  $\chi_Q$  of 2.6 MHz and an asymmetry parameter η of 0.11.

The <sup>27</sup>Al MAS NMR spectra (Figs. 1a–1c) are complex, containing peaks corresponding to tetrahedral, 5-coordinated, and octahedral sites (Smith 1993; MacKenzie and Smith 2002). There is considerable overlap of the peaks and the nature of the structure means that in general there are no well defined second-order quadrupolar line shapes. However, by using spectra

acquired at a range of different magnetic fields (see MacKenzie and Smith 2002), the simulation can be constrained relatively unambiguously. A simulation program was written that allowed a distribution (the Gaussian distribution used here is widely taken as a good first approximation) of the quadrupolar coupling constant to be taken into account. The best set of parameters were taken as those that gave the most consistent set of simulations of the experimental spectra acquired at the fields of 16.45, 14.1, and 8.45 T (Figs. 1a–1c). This simulation was made on the basis of three tetrahedral/5-coordinated and two octahedral sites (the second octahedral site was not included in the simulation of the 8.45 T spectrum, since at this field the resonance is not narrowed at the MAS rates available to be observed). At the higher fields the inclusion of two octahedral peaks is certainly necessary, but this does not preclude the possible presence of a third site, as suggested by the Rietveld analysis. The spectral simulations enable the quadrupole interaction, isotropic chemical shift and relative intensity of each site to be determined, and also allow an estimate to be made of the correction factors for the relative intensities of the tetrahedral and octahedral resonances. The uncorrected site occupancies, derived from the fitted spectra, are 47 ± 3% tetrahedral and 53 ± 3% octahedral. The corrections for

**TABLE 1.** Experimental conditions, crystallographic data, and definitions used in data refinement

Goniometer	Philips X'Pert, Bragg Brentano geometry
Radiation type, source	X-ray, CuKα <sub>1</sub>
Discriminator	primary beam, germanium monochromator
Divergence slit	0.25°
Receiving slit	0.2 mm
Data collection temperature	room temperature
2θ range used in refinement	5–120°
Step size	0.02°
Counting time per step	60 s
Number of reflections	483
Number of parameters varied	62
Space group	C2/m
Chemical composition	Al <sub>4</sub> B <sub>2</sub> O <sub>9</sub>
Z	8
Lattice parameters	$a = 14.8056(7) \text{ \AA}$ , $b = 5.5413(2) \text{ \AA}$ , $c = 15.0531(6) \text{ \AA}$ , $\beta = 90.913(2)^\circ$
Full width at half maximum (Caglioti et al. 1958)	$U = 0.253(16)$ , $V = 0.005(9)$ , $W = 0.0167(11)$

$$\text{FWHM} = \sqrt{U \cdot \tan^2 \theta + V \cdot \tan \theta + W}$$

Durbin-Watson statistic unweighted d(u) and weighted d(w) (Hill and Flack 1987)

$$d(u) = 0.409, d(w) = 0.513$$

$$R_{wp} = \sqrt{\frac{\sum_i (y_{io} - C \cdot y_{ic})^2}{\sum_i w_i y_{io}^2}} \quad 14.9\%$$

$$R_p = \frac{\sum_i |y_{io} - C \cdot y_{ic}|}{\sum_i |y_{io} - y_{ib}|} \quad 16.0\%$$

$$R_e = \sqrt{\frac{N_o - N_p}{\sum_i w_i y_{io}^2}} \quad 2.1\%$$

$$R_B = \frac{\sum_k |I_{ko} - C \cdot I_{kc}|}{\sum_k I_{ko}} \quad 6.6\%$$

Notes:  $y_{io}$ ,  $y_{ic}$ , and  $y_{ib}$  are, respectively, the observed, calculated, and background intensities at step  $i$  in the pattern,  $w_i$  is the observed weight,  $C$  is the scale factor,  $N_o$  is the number of observations (steps),  $N_p$  is the number of parameters varied in the calculated model.  $I_{ko}$  and  $I_{kc}$  are the integrated observed and calculated intensities of reflection  $k$  (Hill and Fischer 1990).

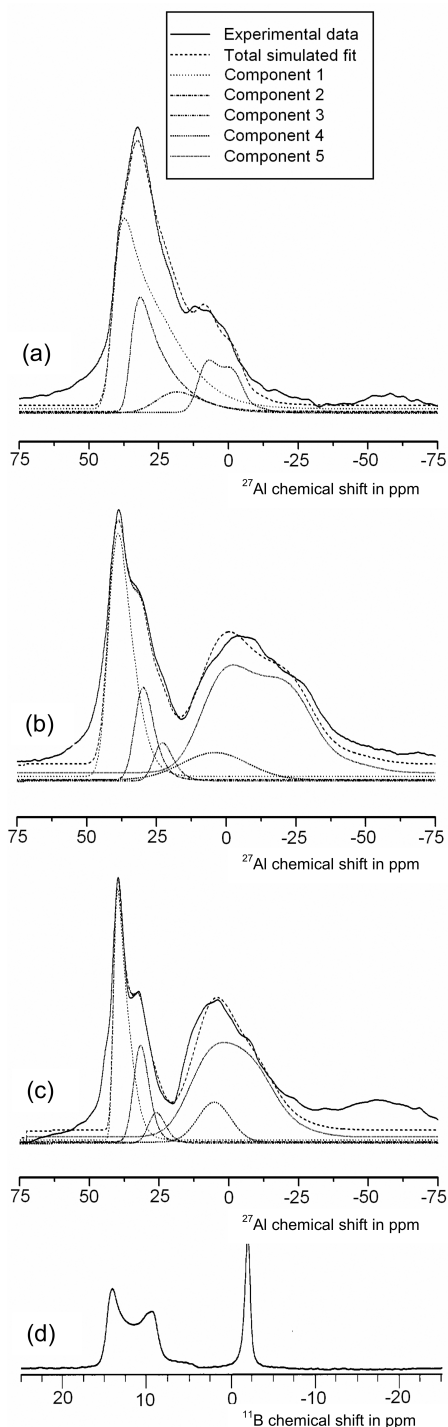


**FIGURE 1.** MAS NMR spectra of sample showing  $^{27}\text{Al}$  MAS NMR at (a) 8.45 T, (b) 14.1 T, (c) 16.45 T, and (d)  $^{11}\text{B}$  MAS NMR at 14.1 T together with the simulations of the  $^{27}\text{Al}$  spectra.

the quadrupolar interactions are less than these errors, except for the second octahedral resonance for which the correction factor is  $\approx 10\%$ . Thus the corrected tetrahedral:octahedral intensity ratio is very close to 50:50. The three fitted sites in the tetrahedral

region have isotropic chemical shifts of  $46.4 \pm 1.2$  ppm (32% mean occupancy),  $51.2 \pm 2.2$  ppm (15% mean occupancy) and  $35.2 \pm 2.2$  ppm (6% mean occupancy). The spectral simulations at all fields indicate that the 46 ppm peak corresponds to a more distorted site, having the largest quadrupole interaction of the tetrahedral sites (8 MHz with a Gaussian distribution width of 20%), compared with 4–6 MHz (with a Gaussian distribution of 25%) for the other two sites.

The octahedral region of the spectrum can be simulated at fields of 14.1 and 16.45 T by peaks with isotropic chemical shifts of  $8.3 \pm 1$  ppm (12% mean occupancy) and  $9.0 \pm 2.2$  ppm (35% mean occupancy). The quadrupole interactions are 4 and 10 MHz respectively, with no distribution necessary; the latter quadrupole interaction is quite large for  $^{27}\text{Al}$  (Smith 1993).

Our careful X-ray diffraction studies showed that the data cannot be indexed based on the metric parameters of mullite as described by Mazza et al. (1992). Neither is the doubling of  $b$  (or  $a$ ) and  $c$  as observed, e.g., for  $\text{Al}_{18}\text{B}_4\text{O}_{33}$  (Ihara et al. 1980; Garsche et al. 1991) sufficient to index all reflections. A structure independent indexing procedure using the program DICVOL (Boultif and Louër 1991) yielded best results for a monoclinic unit cell (Table 1) with the monoclinic angle close to  $90^\circ$  and all three lattice constants doubled relative to the mullite-like parameters reported by Mazza et al. (1992). Systematic extinctions of  $hkl$  reflections with  $h + k \neq 2n$  indicated a C-centered Bravais type. These parameters closely resemble the metric parameters of boralsilite (Grew et al. 1998),  $\text{Al}_6\text{B}_6\text{Si}_2\text{O}_{37}$ , described in the monoclinic space group  $C2/m$  with  $a = 14.77$  Å,  $b = 5.57$  Å,  $c = 15.08$  Å, and  $\beta = 91.96^\circ$  (Peacor et al. 1999; Grew et al. 2008) also represented by its synthetic B-rich counterpart (Grew et al. 2008). Preliminary structure refinements using the atomic parameters of boralsilite gave a reasonable fit with the observed diffraction data and confirmed the close relationship of boralsilite with the aluminum borate studied here. Consequently, the structure determination was performed using the octahedral chain of  $\text{AlO}_6$  groups as the backbone unit in the aluminum borate, which is also the common unit in mullite-type compounds (Fischer and Schneider 2005).

Difference Fourier analyses identified the tetrahedrally coordinated Al and even clearly indicated probable positions for the B atoms, which are normally difficult to determine due to their low scattering power in X-ray diffraction experiments, especially in the powder diffraction refinement. Following this route, the O atoms O1 bridging three Al atoms (Al1, Al2, Al4) and O10 bridging two Al3 and one B2 atom could be located. O10 was determined to reside close to the special position at Wyckoff site  $2b$  and consequently its occupancy was initially set to 50% avoiding unreasonably close distances to itself. However, the refinement yielded coordinates sufficiently separated (O10 – O10 = 2.53 Å) for simultaneous occupancy, but subsequent refinements with full occupancy of the O10 position resulted in an increase of the  $R_{wp}$  value from 18.6 to 21.1% and the  $R_B$  value from 11.7 to 13.8%. Consequently, the occupancy of O10 was constrained to 50% in further refinements. It should be noted that O10 has a distance of 2.12 Å to O7 in the  $\text{Al}_6\text{O}_6$  octahedron that is too close for a reasonable O-O contact. It indicates that the true position of O10 could deviate from the refined position of the disordered atom as further discussed in the discussion section

for  $\text{BO}_3$  and  $\text{BO}_4$  groups.

At this stage, due to the O10 vacancies, the total number of atoms determined corresponded to 32 Al, 16 B, and 70 O atoms per unit cell, thus 4 negative charges corresponding to 2 O atoms are still missing if full occupancies of all cation sites are assumed. It is striking that all positions found in the Fourier analyses can be related to an analogous position in boralsilite except the O5 atom of the boralsilite structure (Peacor et al. 1999; Grew et al. 2008), which resides in Wyckoff site  $2d$  in both the natural and the synthetic compound but is definitely not present in the aluminum borate studied here. The occupancy factor refined to negative values for an O atom in  $0, \frac{1}{2}, \frac{1}{2}$ . To locate scattering matter not determined in the Fourier analyses, a grid search was performed that was introduced by Baur and Fischer (1986) as an alternative tool to the Fourier methods that are biased by termination effects. This method has already been successfully applied to Cr-mullite, where the Cr atom could be located in the octahedral site by both Fourier and grid search analysis (Fischer and Schneider 2000). In the grid search method, as implemented in the BRASS program package, a dummy atom is shifted on a grid within the asymmetric unit of the unit cell, and at each grid position the occupancy of the dummy atom is refined and recorded together with the residuals obtained for these steps. A virtual O atom was shifted on a grid with  $x = 0.00$  to  $0.50$  (step 0.01),  $y = 0.00$  to  $0.24$  (step 0.02), and  $z = 0.00$  to  $1.00$  (step 0.01) yielding 66 963 data points with refined occupancies and residuals. The only remarkable effect in this grid search analysis could be observed in the channel at  $0, y, \frac{1}{2}$  [and symmetrically equivalent at  $\frac{1}{2}, y, \frac{1}{2}$  close to Wyckoff site  $2c$  in  $0, 0, \frac{1}{2}$  (and  $\frac{1}{2}, \frac{1}{2}, \frac{1}{2}$ )]. Figure 2 shows the  $\frac{1}{2}, y, \frac{1}{2}$  path in the three-dimensional grid search map clearly indicating maximum occupation around  $\frac{1}{2}, 0.4, \frac{1}{2}$  with lowest residual at  $\frac{1}{2}, \frac{1}{2}, \frac{1}{2}$ . Subsequent refinement with all parameters varied simultaneously showed a preference for the split position. It should be noted that in the grid search analyses occupancies and residuals vary within small margins only which is due to the fact that only 2 parameters (occupancy and scale factor) are refined and all other parameters are fixed. The actual improvement of the refinement after introducing the O5' split position is much more pronounced, yielding an occupancy of 0.194(7) corresponding to 1.6 atoms per unit cell. Considering that the accuracy of refining split positions in Rietveld refinements is low, the occupancy is close to the 2 O atoms needed for charge compensation.

Finally, the occupancy was fixed to 2 atoms per unit cell. However, this position cannot be interpreted as a normal bridging atom between two adjacent Al and/or B atoms. The distance to B1 of 1.8 Å is too long for a normal bond as well as the distance of 2.9 Å to the next Al1 atom. If the results of the grid search analysis are considered to be significant, O5' most likely represents the oxygen atoms needed for charge compensation. As a final check of the unfavorable solution of introducing the O5' atom and constraining the occupancy of O10 to 50%, a refinement was performed with fully occupied O10 and omitted O5'. The  $R_B$  value immediately increased from 6.6 to 10.5% with remarkable effects in the powder diffraction diagram showing a misfit especially in the low  $2\theta$  region. Further explanations are given in the discussion section.

All refinements were performed without constraints on the

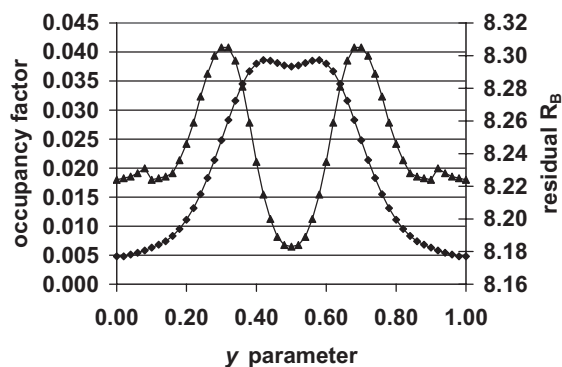


FIGURE 2. Results of the grid search analysis on the path along  $\frac{1}{2}, y, \frac{1}{2}$ . Squares represent occupancy factors (left ordinate), triangles represent  $R_B$  values (right ordinate).

atomic parameters. Only the displacement parameters were constrained to be equal within groups of atoms. The final residuals (Table 1) are high but in the normal range obtained for well crystalline samples with low background as discussed by Hill and Fischer (1990) if an empirical pseudo-Voigt function is used. Final atomic parameters<sup>1</sup> are listed in Table 2 together with the corresponding parameters of boralsilite (Peacor et al. 1999). Selected interatomic distances are listed in Table 3. The fit between observed and calculated intensities after the last cycle of refinements is shown in Figure 3.

## DISCUSSION

### The Al-B distribution in $\text{Al}_4\text{B}_2\text{O}_9$

Assuming full occupancies of the cation sites, the crystal-structure refinement yielded 16 octahedrally coordinated Al atoms residing on three sites, and 16 four- and five-coordinated Al atoms on four sites. The 16 B atoms are located in four positions, two of which (B2 and B3) are disordered, split into three and four-coordinated sites, the other two B atoms (B1 and B4) are exclusively three-coordinated.

The NMR data confirm the essential details of the structure, including the ratio of octahedral:tetrahedral sites (~50:50), the ratio of  $\text{BO}_3$  to  $\text{BO}_4$  units (~80:20) and the presence of multiple tetrahedral and octahedral Al sites. The NMR determination of the  $\text{BO}_3$ : $\text{BO}_4$  ratio is robust, being based on direct spectral integration. The octahedral:tetrahedral Al ratio and the partitioning of the Al between the various tetrahedral sites is equally robust, having been derived from consistent simulations of the spectral data at three magnetic fields, taking into account the distribution of quadrupolar interactions.

<sup>1</sup> Deposit item AM-08-026, CIF. Deposit items are available two ways: For a paper copy contact the Business Office of the Mineralogical Society of America (see inside front cover of recent issue) for price information. For an electronic copy visit the MSA web site at <http://www.minsocam.org>, go to the American Mineralogist Contents, find the table of contents for the specific volume/issue wanted, and then click on the deposit link there.

**TABLE 2.** Positional parameters, isotropic displacement factors ( $\text{\AA}^2$ ), site symmetries, Wyckoff positions, and occupancies (first line:  $\text{Al}_4\text{B}_2\text{O}_9$ , second line: boralsilite)

Full name	x	y	z	B ( $\text{\AA}^2$ )	Site symm.	Wyckoff pos.	No. of atoms per unit cell
Al1	0.8631(6)	0	0.3409(6)	0.43(3)	<i>m</i>	4 <i>i</i>	4
	0.86873(7)	0	0.33837(7)	0.42(2)			
Al2	0.8147(6)	0	0.1622(6)	0.43(3)	<i>m</i>	4 <i>i</i>	4
	0.81194(7)	0	0.15838(7)	0.40(2)			
Al3	0.5696(6)	0	0.0675(6)	0.43(3)	<i>m</i>	4 <i>i</i>	4
	0.57170(7)	0	0.06951(7)	0.51(2)			
Al4	0.6739(7)	0	0.3439(6)	0.43(3)	<i>m</i>	4 <i>i</i>	4
	0.67697(7)	0	0.34140(7)	0.40(2)			
Al5	0.0002(6)	0.7471(16)	0.2480(5)	0.43(3)	1	8 <i>j</i>	8
	0.00396(5)	0.74670(13)	0.24322(5)	0.43(1)			
Al6	¼	¼	0	0.43(3)	1	4 <i>e</i>	4
	¼	¼	0	0.39(2)			
Al7	¼	¼	½	0.43(3)	1	4 <i>f</i>	4
	¼	¼	½	0.41(2)			
B1	0.1026(20)	0	0.1053(19)	0.4(3)	<i>m</i>	4 <i>i</i>	4
	0.1018(3)	0	0.1009(3)	0.66(7)			
B2	0.3789(23)	0	0.1382(21)	0.4(3)	<i>m</i>	4 <i>i</i>	4
	0.3774(3)	0	0.1192(3)	0.69(7)			
B3	0.1352(25)	0	0.3662(20)	0.4(3)	<i>m</i>	4 <i>i</i>	4
	0.1356(3)	0	0.3633(3)	0.54(7)			
B4	0.3896(22)	0	0.4005(19)	0.4(3)	<i>m</i>	4 <i>i</i>	4
	Si	0.42541(7)	0	0.41917(7)			
O1	0.7563(13)	0	0.2561(10)	0.73(7)	<i>m</i>	4 <i>i</i>	4
	0.7658(2)	0	0.2671(2)	0.59(4)			
O2	0.7979(11)	0	0.4445(10)	0.73(7)	<i>m</i>	4 <i>i</i>	4
	0.7965(2)	0	0.4340(2)	0.53(4)			
O3	0.9245(12)	0	0.2152(8)	0.73(7)	<i>m</i>	4 <i>i</i>	4
	0.9244(2)	0	0.2214(2)	0.41(4)			
O4	0.9226(6)	0.7157(20)	0.3536(6)	0.73(7)	1	8 <i>j</i>	8
	0.9355(1)	0.7387(3)	0.3573(1)	0.63(3)			
O5'	0.0332(19)	0	0.4376(16)	0.73(7)	<i>m</i>	4 <i>i</i>	2
O5	0	½	½	0.90(7)	2/ <i>m</i>	2 <i>d</i>	2
	0.3221(11)	0	0.4562(10)	0.73(7)			
O6	0.3234(2)	0	0.4584(2)	0.55(4)	<i>m</i>	4 <i>i</i>	4
	0.8261(7)	0.7183(18)	0.0993(5)	0.73(7)			
O7	0.8208(1)	0.7151(4)	0.1063(1)	0.57(3)	1	8 <i>j</i>	8
	0.6967(12)	0	0.0682(9)	0.73(7)			
O8	0.6973(2)	0	0.0613(2)	0.49(4)	<i>m</i>	4 <i>i</i>	4
	0.0663(7)	0.7711(22)	0.1310(6)	0.73(7)			
O9	0.0680(1)	0.7843(3)	0.1333(1)	0.58(3)	1	8 <i>j</i>	8
	0.4300(20)	0	0.0474(19)	0.73(7)			
O10A	0.4444(2)	0	0.0494(2)	0.98(5)	<i>m</i>	4 <i>i</i>	3.80(3)
O10B	½	0	0	2.7(7)	2/ <i>m</i>	2 <i>b</i>	0.29(2)
O11	0.6734(6)	0.2852(20)	0.3953(5)	0.73(7)	1	8 <i>j</i>	8
	0.6678(1)	0.2877(4)	0.3991(1)	0.57(3)			
O12	0.5766(12)	0	0.2751(9)	0.73(7)	<i>m</i>	4 <i>i</i>	4
	0.5757(2)	0	0.2812(4)	0.50(4)			
O13	0.4362(11)	0	0.1981(9)	0.73(7)	<i>m</i>	4 <i>i</i>	4
	0.4313(2)	0	0.2005(2)	0.57(4)			
O14	0.0659(11)	0	0.2919(9)	0.73(7)	<i>m</i>	4 <i>i</i>	4
	0.0767(2)	0	0.2927(2)	0.49(4)			
O15	0.8242(10)	0	0.9558(10)	0.73(7)	<i>m</i>	4 <i>i</i>	4
	0.8314(2)	0	0.9594(2)	0.51(4)			

Notes: Data for site symmetry and Wyckoff position taken from *International Tables of Crystallography* (Hahn 2002). Atomic parameters for boralsilite from Peacor et al. (1999).

### Structural relationships with boralsilite

The crystal structure of  $\text{Al}_4\text{B}_2\text{O}_9$  is closely related to the structures of boralsilite,  $\text{Al}_{16}\text{B}_6\text{Si}_2\text{O}_{37}$  (Peacor et al. 1999; Grew et al. 2008) characterized by the chains of edge sharing  $\text{AlO}_6$ -octahedra crosslinked by  $\text{SiO}_4$ ,  $\text{AlO}_4$ ,  $\text{AlO}_5$ ,  $\text{BO}_3$ , and  $\text{BO}_4$  groups. The structure determination presented here confirms the composition  $\text{Al}_{32}\text{B}_{16}\text{O}_{72}$  obtained by chemical analysis, which corresponds to  $\text{Al}_4\text{B}_2\text{O}_9$  described by Mazza et al. (1992). However, the compound crystallizes in the subgroup of *Pbam* with index 8 by doubling all three lattice constants accompanied by a small monoclinic distortion as observed for boralsilite. This deviates from the description given by Mazza et al. (1992), who described the aluminum borates in the *Pbam* supergroup with pseudo-tetragonal metric.

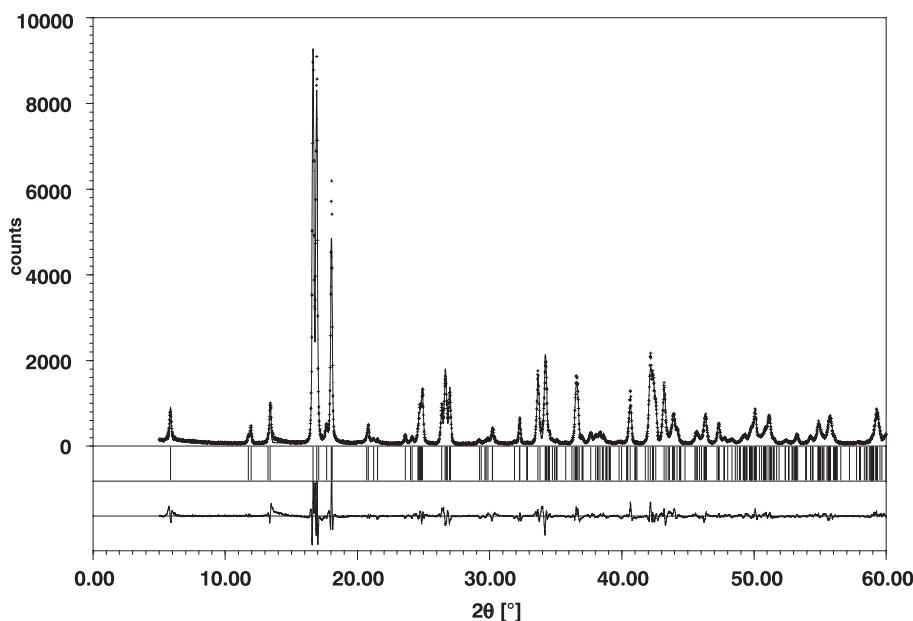
The crystal structures of  $\text{Al}_4\text{B}_2\text{O}_9$  and boralsilite are shown in Figures 4 and 5. Considering that the boralsilite structure has been refined from single-crystal data by Peacor et al. (1999), the results of the Rietveld refinement of the aluminum borate reasonably well agrees with it. Just the estimated standard deviations are about 5 to 6 times higher in the powder diffraction refinement. Even the B atoms could be located and refined without constraints. The main difference between the two structures lies: (1) in the replacement of Si in boralsilite by B in the aluminum borate assuming a nearly planar 3-coordination; (2) in the disordered distribution of O5' atoms in the 0, *y*, ½ and ½, *y*, ½ (Fig. 4) channels in the aluminum borate; and (3) in the preference of some Al atoms to achieve fivefold coordination, which is more pronounced in boralsilite.

**TABLE 3.** Selected interatomic distances ( $\text{\AA}$ )

<b><math>\text{AlO}_6</math> octahedra</b>								
Al5			Al6			Al7		
O13	1.820(13)	1.846(2)	2×O7	1.866(9)	1.894(2)	2×O2	1.772(10)	1.858(2)
O12	1.819(14)	1.816(2)	2×O15	1.895(10)	1.953(2)	2×O6	1.875(11)	1.886(2)
O14	1.824(13)	1.910(2)	2×O8	1.903(10)	1.857(2)	2×O11	1.937(8)	1.926(2)
O3	1.856(14)	1.859(2)						
O4	1.984(12)	2.025(2)						
O9	2.032(12)	1.947(2)						
mean 6	1.889	1.900	mean 6	1.888	1.901	mean 6	1.861	1.890
<b><math>\text{AlO}_4</math> and <math>\text{AlO}_5</math> groups</b>								
Al1	1.813(11)	1.776(2)	Al2			Al3		
2×O4	1.847(17)	1.822(3)	O1	1.668(19)	1.796(3)	O10	1.730(30)	1.801(3)
O2	2.017(19)	1.831(3)	O3	1.801(19)	1.885(3)	2×O9	1.782(12)	1.856(2)
O1	2.112(15)	1.971(3)	2×O7	1.835(11)	1.779(2)	O8	1.882(20)	1.864(3)
O3			O8	2.231(18)	2.200(3)	O10	2.084(30)	1.894(3)
mean 5	1.920	1.835	mean 4	1.785	1.810	mean 4*	1.794	1.844
			mean 5	1.874	1.888	or*	1.883	1.868
Al4								
O12	1.759(19)	1.723(3)						
2×O11	1.760(11)	1.831(2)						
O1	1.813(20)	1.754(3)						
O2	2.361	2.213(3)						
mean 4	1.773	1.785						
mean 5	1.891	1.870						
<b><math>\text{BO}_3</math> and <math>\text{BO}_4</math> groups</b>								
B1			B2			B3		
O15	1.43(3)	1.364(5)	O13	1.23(3)	1.439(5)	2×O11	1.39(2)	1.379(3)
2×O9	1.43(2)	1.397(3)	2×O7	1.55(2)	1.470(3)	O14	1.51(4)	1.351(5)
			O10	1.57(4)	1.469(5)	O5'	[1.87(4)]	
mean 3	1.43	1.386	mean 4	1.48	1.462	mean 3	1.43	1.370
B4		Si						
O6	1.32(3)	1.637(3)						
2×O4	1.48(2)	1.635(2)						
O5		1.615(1)						
mean 3	1.43							
mean 4		1.630						

Notes: First column =  $\text{Al}_4\text{B}_2\text{O}_9$ ; second column = boralsilite.

\* Mean values are given alternatively for the small and the large Al3-O10 distance.

**FIGURE 3.** Observed (crosses) and calculated (solid line) powder patterns with difference curves underneath. Peak positions permitted by the cell metric are indicated by tick marks.

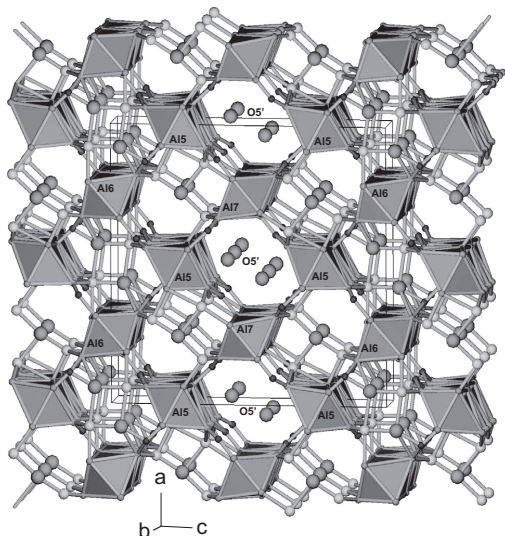


**FIGURE 4.** Projection of the crystal structure of  $\text{Al}_4\text{B}_2\text{O}_9$ . Small circles represent B atoms, medium-sized circles are Al atoms, and big circles represent O atoms outside of the octahedral chain. Projection parallel **b** rotated by  $4^\circ$  about **a** and **a**  $\times$  **b**.

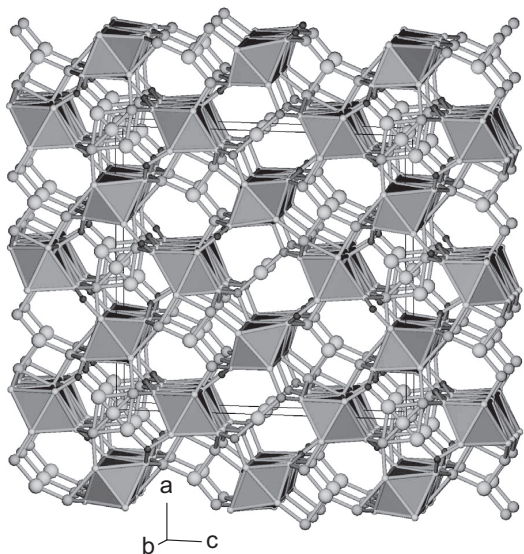


**FIGURE 5.** Projection of the crystal structure of boralsilite after Peacor et al. (1999). Assignment of atoms and orientation as in Figure 4.

silite. Furthermore, it is assumed here that the O4 atom bridges Al atoms exclusively, whereas the O atom in boralsilite alternatively bridges Al atoms (O10A in Peacor et al. 1999), or B atoms (O10B) forming  $\text{B}_2\text{O}_7$  groups with partial occupancies for O10A and O10B corresponding to the coordinated Al and B atoms. The latter model corresponds to a hypothetical “paraboralsilite” structure described by Peacor et al. (1999). Such a configuration could not be resolved for the  $\text{Al}_4\text{B}_2\text{O}_9$  studied here but could be present in minor amounts not detectable in the powder diffraction data.

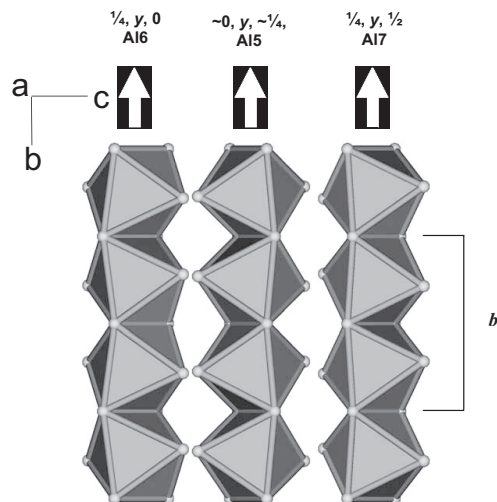


**FIGURE 6.** The octahedral chains parallel **b**. Projection parallel **a**.

### The octahedral chains

Similar to mullite-type structures, the octahedral axes through the nonbridging O atoms always point to the edges of neighboring octahedra that yields the highest possible topological symmetry in the tetragonal space group (Fischer and Schneider 2005). Various linkages of the octahedral chains via O bridges in the channels with  $\text{SiO}_-$ ,  $\text{AlO}_-$ , and  $\text{BO}_-$  units yields orthorhombic mullite or the monoclinic structures of boralsilite and the aluminum borate studied here. Projections of the three symmetrically independent chains (Al5 in  $\sim 0, y, \sim 1/4$ ; Al6 in  $1/4, y, 0$ ; Al7 in  $1/4, y, 1/2$ ) are shown in Figure 6. This arrangement defines the length of the **b** unit-cell edge that is a multiple of the octahedral edge in chain direction with small deviations due to some tilting in the octahedral chains in lower symmetries. The interatomic distances agree well with the values expected from the sum of the ionic radii (Shannon 1976), which is 1.886 Å for  $^{VI}\text{Al}$  and  $^{III}\text{O}$ . Just the mean distances in the Al7 octahedron are considerably smaller due to the small distances to O2 of 1.772 Å. The distortion index (DI) of these sites (the mean angular deviation from ideal octahedral symmetry), calculated from the Rietveld structural refinement, indicates that the distortion of Al6 (DI = 3.06) is slightly smaller than the distortions of Al7 and Al5 (5.37 and 4.87, respectively). The fitted octahedral region of the  $^{27}\text{Al}$  NMR spectra at the higher fields (Fig. 1) indicates two sites (although the presence of three cannot be ruled out). The mean NMR site occupancies derived from the spectral simulations at the higher fields (expressed in terms of the total octahedral and tetrahedral Al content) are about 12 and 35%, the latter corresponding to a more distorted environment. The correspondence between these sites and the three octahedral Al sites of the Rietveld refinement is not immediately obvious, but one possible assignment is that the more populated and more distorted NMR site represents a combination of Al5 and Al7 (Rietveld occupancy 37.5%), whereas the less populated NMR site represents Al6 (Rietveld occupancy 12.5%). This suggestion is also consistent with the Rietveld distortion parameters for these sites.

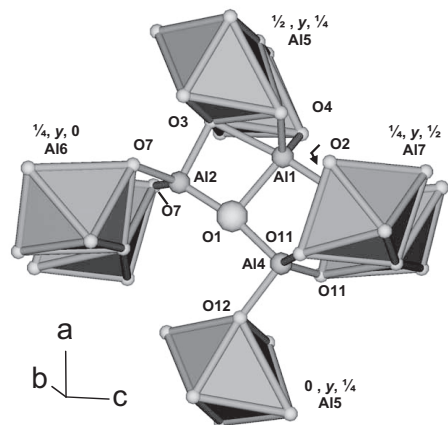


FIGURE 7. Linkage of chains in the  $\frac{1}{4}, y, \frac{1}{4}$  channel. Projection parallel **b**, rotated by  $10^\circ$  about **a** and **a**  $\times$  **b**.

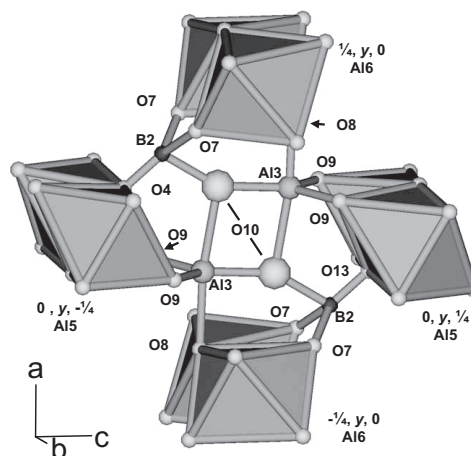


FIGURE 8. Linkage of chains in the  $0, y, 0$  channel. Projection parallel **b**, rotated by  $10^\circ$  about **a** and **a**  $\times$  **b**.

#### $\text{AlO}_4$ and $\text{AlO}_5$ groups

The local structures of the 4- and 5-coordinated Al atoms are shown in Figures 7 and 8. Al1, Al2, and Al4 atoms are bridging neighboring octahedra and are linked together via the O1 atom in the  $\frac{1}{4}, y, \frac{1}{4}$  channel as shown in Figure 7. The Al1 atom is clearly 5-coordinated, whereas Al2 and Al4 have a preference to a 4-coordination with an additional bond to O8 and O2, respectively. The Al3 atom has three bonds to the neighboring octahedral chains and another bond to one of the two O10 atoms in the  $0, y, 0$  channel as shown in Figure 8. It cannot be linked to both O10 atoms because they cannot be occupied simultaneously due to their close distance. Therefore, O10 can only be half occupied and Al3 is statistically bonded to just one of the two O10 atoms either with a short distance of 1.73 Å or a long distance of 2.08 Å. The simulations of the  $^{27}\text{Al}$  NMR spectra only distinguish three non-octahedral resonances, the isotropic chemical shifts of which show slight variations at the different fields. One resonance, at 46.4 ppm, has a mean occupancy (relative to the total Al content) of 32%, while the second, at 51.2 ppm has a mean occupancy of 15%. The third resonance, at 35.2 ppm has a much lower mean occupancy (6%); the isotropic shift of this site suggests that it may be associated with the 5-coordinated Al1 site, although this NMR occupancy accounts for only about 1/3 of the Al1 atoms as indicated by the Rietveld refinement. The most highly populated  $^{27}\text{Al}$  resonance at 46.4 ppm is also the most distorted, with a quadrupole interaction of 8 MHz. On the basis of site occupancies, this resonance must be associated with more than one Al site, the most likely candidates being Al3 and Al2, since these are the most distorted of the tetrahedral sites, with tetrahedral distortion indices (DI) of 20.4 and 10.6, respectively, calculated from the relevant interatomic angles. The combined occupancy of these two sites according to the Rietveld refinement (25%) is in only fair agreement with the mean NMR occupancy of about 32%. If this assignment is accepted, the remaining tetrahedral resonance at 51.2 ppm would be associated with Al4, which has a Rietveld occupancy of 12.5%, in reasonable agreement with the mean NMR occupancy of 15%.

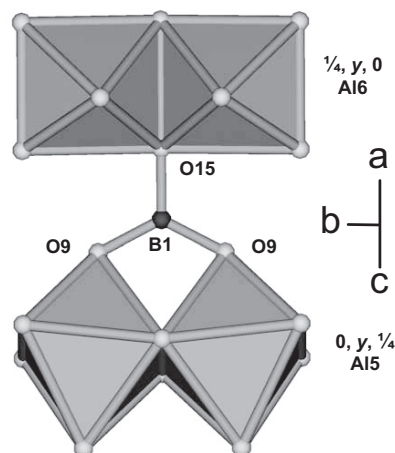


FIGURE 9. The coordination of B1. Projection parallel [101].

#### $\text{BO}_3$ and $\text{BO}_4$ groups

The B atoms reside in the central positions linking two nonbridging O atoms of an octahedral chain with a bridging O atom of a neighboring chain as shown in Figures 8 to 11. B2 can have an additional bond to O10 (Fig. 8) and consequently will be shifted slightly toward the O10 atom to achieve a more regular tetrahedral coordination. This cannot be verified in the Rietveld refinement, which just shows the ordered position of B2 in its nearly planar 3-coordination. However, it clearly emerges from the statistical distribution of the O10 atoms that there is always one of the two adjacent B2 atoms in trigonal planar coordination while the other one is in tetrahedral coordination. The statistical distribution of B2 atoms on trigonal and tetrahedral sites could explain the unfavorable O10-O7 distances if we assume that the O10 atom is slightly shifted toward the B2 position to compensate for the electron density assigned to tetrahedrally coordinated B2 above the plane of the  $\text{BO}_3$  group formed by B2,  $2 \times \text{O7}$ , and O13 (Fig. 8). In other words, introducing a

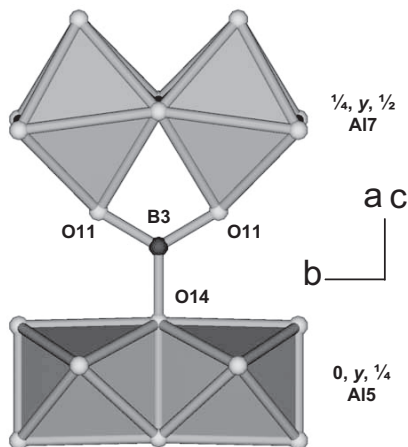


FIGURE 10. The coordination of B3. Projection parallel  $[\bar{1}01]$ .

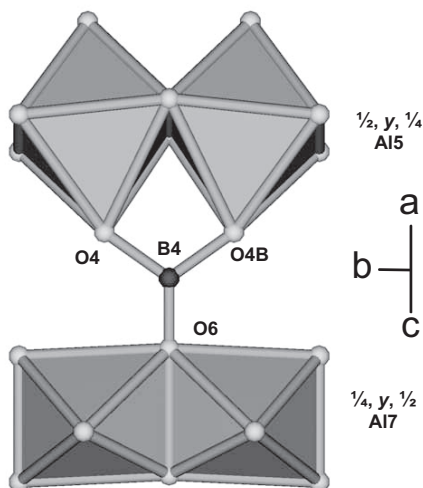


FIGURE 11. The coordination of B4. Projection parallel  $[101]$ .

split B2 position would “push” the O10 atom toward the  $0, \frac{1}{2}, 0$  position (Wyckoff position  $2b$ ) and thus further away from O7. The  $^{11}\text{B}$  NMR spectra clearly indicate the presence of boron in both tetrahedral coordination (site B2) and trigonal coordination (sites B1, B3, and B4), the latter, however, are too similar to be distinguished by NMR. It should be noted that the NMR site occupancy is consistent with the Rietveld results.

The mean B-O distances are in good agreement with those reported for single crystals of boralsilite (Peacor et al. 1999) to within  $0.06 \text{ \AA}$ , which is good for a Rietveld refinement without applying restraints on bond distances. As a result of their low scattering power, B positions are extremely difficult to determine and to refine based on X-ray powder diffraction data.

#### O5' in the $0, y, \frac{1}{2}$ and $\frac{1}{2}, y, \frac{1}{2}$ channels

In contrast to boralsilite where the O5 atom bridges two adjacent Si atoms in the  $0, y, \frac{1}{2}$  channel (Fig. 5), the Si-O5-Si bridge is missing in the aluminum borate structure (Fig. 4). As stated

in the results section, a grid search analysis yielded a position close to  $\frac{1}{2}, \frac{1}{2}, \frac{1}{2}$  as the only significant electron density not yet determined in the whole unit cell. Both the grid search analysis and Rietveld refinement indicated that the position is split into two sites shifted toward the B3 atoms as close as  $1.87 \text{ \AA}$ . This suggests that the situation could be similar to the configuration described above for B2 and O4 where we expect a shift of the B atom toward the O atom in going from 3- to 4-coordination. This may be assumed for B3 and O5' as well. However, in that case O5' would be a terminating atom with no further bridging to another cation that is unlikely. We therefore consider the O5' atom as a representative of scattering matter in the channel that cannot be assigned to a well defined position and that just converged in a local minimum in the Rietveld refinement. The lowering of the  $R_B$  value of about 0.7% upon introducing this position and the fact that indeed two more O atoms are needed for charge compensation are strong indicators to believe that the O atoms are located in this channel. They are probably highly disordered causing local dislocations of the B atoms, which reside on the inside walls of the elliptical channels.

If the electron density represented by O5' would not be considered, Al and/or B vacancies could be assumed to compensate for the reduced O contents. Vacancies statistically distributed over the Al and B sites would not be detectable in the Rietveld refinement of such a complex crystal structure. However, partially occupied cation sites would be possible for all sites outside the octahedral chain based on crystal chemical considerations. Accordingly, the chemical composition would be  $\text{Al}_{31.12}\text{B}_{15.56}\text{O}_{70}$  (or  $\text{Al}_{30.85}\text{B}_{15.82}\text{O}_{70}$  based on an Al/B ratio of 1.95), which can be written as  $\text{Al}_{16}\text{Al}_{15.12}\text{B}_{15.56}\text{O}_{70}$  if the 16 Al atoms in the octahedral chains are separated. Consequently, vacancies corresponding to 0.88 Al and 0.44 B atoms would be distributed over four Al sites and four B sites.

Based on crystal chemical considerations, a model with a fully occupied O10 site and vacant O5' positions definitely would be more favorable. The Rietveld refinements might not be suitable to resolve these details in such a complex structure. Work is in progress to synthesize single crystals of sufficient size and quality, which could not be achieved so far.

#### ACKNOWLEDGMENTS

We thank Hannes Krüger and Michael Wendschuh for their experimental assistance with the X-ray diffraction experiments, T. Kemp for his assistance in simulating the  $^{27}\text{Al}$  MAS NMR spectra, an anonymous referee for comments on an earlier version of the manuscript, and Heribert Graetsch and Andrew Locoek for their comments on the current manuscript, as well as Edward Grew for his detailed suggestions and for sending us a preprint on natural and synthetic boralsilite.

#### REFERENCES CITED

- Baur, W.H. and Fischer, R.X. (1986) Recognition and treatment of background problems in neutron powder diffraction refinements. In C.S. Barrett, J.B. Cohen, J. Faber, R. Jenkins, D.E. Leyden, J.C. Russ, and P.K. Predecki, Eds., *Advances in X-ray Analysis*, 29, p. 131–142. Plenum Publishing Corporation, New York.
- Birkenstock, J., Fischer, R.X., and Messner, T. (2007) BRASS, The Bremen Rietveld Analysis and Structure Suite. Fachbereich Geowissenschaften Universität Bremen, Germany.
- Boultif, A. and Louër, D. (1991) Indexing of powder diffraction patterns for low-symmetry lattices by the successive dichotomy method. *Journal of Applied Crystallography*, 24, 987–993.
- Caglioti, G., Paoletti, A., and Ricci, F.P. (1958) Choice of collimators for a crystal spectrometer for neutron diffraction. *Nuclear Instruments*, 3, 223–228.
- Fischer, R.X. and Messner, T. (2007) STRUPLO, a new version of the structure

- drawing program. Fachbereich Geowissenschaften Universität Bremen, Germany.
- Fischer, R.X. and Schneider, H. (2000) Crystal structure of Cr-mullite. *American Mineralogist*, 85, 1175–1179.
- (2005) The mullite-type family of crystal structures. In H. Schneider and S. Komarneni, Eds., *Mullite*, p. 1–46, 128–141. Wiley-VCH, Weinheim.
- Fischer, R.X., Lengauer, C., Tillmanns, E., Ensink, R.J., Reiss, C.A., and Fantner, E.J. (1993) PC-Rietveld plus, a comprehensive Rietveld analysis package for PC. *Materials Science Forum*, 133–136, 287–292.
- Gajhede, M., Larsen, S., and Rettrup, S. (1986) Electron density of orthoboric acid determined by X-ray diffraction at 105 K and ab initio calculations. *Acta Crystallographica*, B42, 545–552.
- Garsche, M., Tillmanns, E., Almen, H., Schneider, H., and Kupčik, V. (1991) Incorporation of chromium into aluminium borate  $9\text{Al}_2\text{O}_3 \cdot 2\text{B}_2\text{O}_3 (\text{A}_9\text{B}_2)$ . *European Journal of Mineralogy*, 3, 793–808.
- Grew, E.S., McGee, J.J., Yates, M.G., Peacor, D.R., Rouse, R.C., Huijsmans, J.P.P., Shearer, C.K., Wiedenbeck, M., Thost, D.E., and Su, S.C. (1998) Boralsilite ( $\text{Al}_{16}\text{B}_8\text{Si}_2\text{O}_{37}$ ): A new mineral related to sillimanite from pegmatites in granulite-facies rocks. *American Mineralogist*, 83, 638–651.
- Grew, E.S., Graetsch, H.A., Pöter, B., Yates, M.G., Buick, I., Bernhardt, H.-J., Schreyer, W., Werding, G., Carson, C.J., and Clarke, G.L. (2008) Boralsilite,  $\text{Al}_{16}\text{B}_8\text{Si}_2\text{O}_{37}$ , and “boron-mullite”: compositional variations and associated phases in experiment and nature. *American Mineralogist*, 93, 283–299.
- Hahn, T. (2002) *International Tables for Crystallography*, vol. A. Kluwer, Dordrecht, The Netherlands.
- Hill, R.J. and Fischer, R.X. (1990) Profile agreement indices in Rietveld and pattern-fitting analysis. *Journal of Applied Crystallography*, 23, 462–468.
- Hill, R.J. and Flack, H.D. (1987) The use of the Durbin-Watson *d* statistic in Rietveld analysis. *Journal of Applied Crystallography*, 20, 356–361.
- Hovestreydt, E. (1983) On the atomic scattering factor for  $\text{O}^{2-}$ . *Acta Crystallographica*, A39, 268–269.
- Ibers, J.A. and Hamilton, W.C. (1974) *International Tables for X-ray Crystallography*, vol. 4, p. 99–149. Kynoch, Birmingham, U.K.
- Ihara, M., Imai, K., Fukunaga, J., and Yoshida, N. (1980) Crystal structure of borooaluminate,  $9\text{Al}_2\text{O}_3 \cdot 2\text{B}_2\text{O}_3$ . *Yogyo Kyokai Shi*, 88, 77–84 (in Japanese with English abstract).
- MacKenzie, K.J.D. and Smith, M.E. (2002) Multinuclear Solid-State NMR of Inorganic Materials, vol. 6. Pergamon Materials Series, Pergamon-Elsevier, Oxford.
- Mazza, D., Vallino, M., and Busca, G. (1992) Mullite-type structures in the systems  $\text{Al}_2\text{O}_3\text{-Me}_2\text{O}$  (Me = Na, K) and  $\text{Al}_2\text{O}_3\text{-B}_2\text{O}_3$ . *Journal of the American Ceramic Society*, 75, 1929–1934.
- Peacor, D.R., Rouse, R.C., and Grew, E.S. (1999) Crystal structure of boralsilite and its relation to a family of borooaluminosilicates, sillimanite, and andalusite. *American Mineralogist*, 84, 1152–1161.
- Prince, E. (1995) Mathematical aspects of Rietveld refinement. In R.A. Young, Ed., *The Rietveld Method*, p. 43–54. International Union of Crystallography, Oxford University Press, U.K.
- Rietveld, H.M. (1969) A profile refinement method for nuclear and magnetic structures. *Journal of Applied Crystallography*, 2, 65–71.
- Scholze, H. (1956) Über Aluminiumborate. *Zeitschrift für anorganische und allgemeine Chemie*, 284, 272–277.
- Shannon, R.D. (1976) Revised effective ionic radii and systematic studies of interatomic distances in halides and chalcogenides. *Acta Crystallographica*, A 32, 751–767.
- Smith, M.E. (1993) Application of  $^{27}\text{Al}$  NMR techniques to structure determination in solids. *Applied Magnetic Resonance*, 4, 1–64.
- Smith, M.E. and van Eck, E.R.H. (1999) Recent advances in experimental solid state NMR methodology for half-integer spin quadrupolar nuclei. *Progress in Nuclear Magnetic Resonance Spectroscopy*, 34, 159–201.
- Werdning, G. and Schreyer, W. (1984) Alkali-free tourmaline in the system  $\text{MgO-Al}_2\text{O}_3\text{-SiO}_2\text{-B}_2\text{O}_3\text{-H}_2\text{O}$ . *Geochimica Cosmochimica Acta*, 48, 1331–1344.
- (1990) Synthetic dumortierite: its *PtX*-dependent compositional variations in the system  $\text{Al}_2\text{O}_3\text{-B}_2\text{O}_3\text{-SiO}_2\text{-H}_2\text{O}$ . *Contributions to Mineralogy and Petrology*, 105, 11–24.
- (1996) Experimental studies on borosilicates and selected borates. In L.M. Anovitz and E.S. Grew, Eds., *Boron: Mineralogy, Petrology and Geochemistry*, 33, p. 117–163. Reviews in Mineralogy, Mineralogical Society of America, Chantilly, Virginia.

MANUSCRIPT RECEIVED JULY 19, 2007

MANUSCRIPT ACCEPTED DECEMBER 26, 2007

MANUSCRIPT HANDLED BY EDWARD GREW